Performance of Neutral Point Clamped Five Level Inverter Using Space Vector Modulation Control Fed by DPC-VF-SVM Rectifier

DJAMILA CHERIFI
Department of Electrical Engineering University of Dr.Tahar Moulay
P. O. B. 138, 20000 Ennasr, Saida
ALGERIA

YAHIA MILOUD
Department of Electrical Engineering University of Dr.Tahar Moulay
P. O. B. 138, 20000 Ennasr, Saida
ALGERIA

MOHAMED MOSTEFAI
Department of Electrical Engineering University of Dr.Tahar Moulay
P. O. B. 138, 20000 Ennasr, Saida
ALGERIA

Abstract: - The purpose of this paper is to develop a control and regulation method for the input DC voltage of a five level neutral point clamping (NPC) inverter feeding a induction motor. In this context, the authors propose in the first part, the control strategy of three-phase pulse width modulation rectifier, they propose the virtual flux-based direct control (DPC_VF) with vector modulation (SVM), this method is applied for the enhancement of network power quality by compensation of harmonic currents produced by an non linear load, and good regulation of DC-bus voltage. The second part of the paper is dedicated to the presentation of the model of the three phase, five-level NPC voltage source inverter with its space vector modulation (SVM) control method. The performance of the proposed strategy in terms of out-put voltage and THD has studied successfully and shown using MATLAB/Simulink.

Key-Words: - Diode-clamped five level inverter, direct power control (DPC), PWM rectifier, space vector modulation (SVM), virtual flux.

Received: April 20, 2021. Revised: October 5, 2021. Accepted: October 29, 2021. Published: November 20, 2021.

1 Introduction

Inverters are widely used in various industrial applications such as power conditioning system for renewable energy and variable speed drives system because of their ability to control the magnitude and frequency of the output voltage, [1], [2], [3]. The use of a conventional two-level inverter in the field of high power applications is not appropriate because numerous industrial applications have begun to require high power apparatus in recent years, [4]. Some medium voltage drives and utility applications require medium voltage and megawatt power level .For a medium voltage grid, it is troublesome to connect only one power semiconductor switch directly, also for reduce the harmonics in the inverter output voltage and to meet the voltage rating of the power devices the multi-level structures are used as an alternative in high power and medium voltage situations, [5], [6].

The concept of multilevel inverter has been introduced since 1970. the research was able to face the handicaps presented by the classical structure, the term multilevel began with three level converter subsequently several multilevel converter topologies has been developed, such as floating diode, floating-capacitor, and cascaded inverters. The aims of these structures are make to generate an output voltage of several levels and to improve the quality of the output voltage, as well as to overcome the problems associated with two-level inverters, [7], [8], [9], [10]. However, the multilevel inverters can be developed by either using multiple 3-phase bridges or by increasing the number of switching devices per phase, in order to increase the number of levels, [11].The advantages of multilevel inverter are the dv/dt stresses on the switching devices are reduced due to the small increment in voltage steps, reduced electromagnetic compatibility (EMC) when operated at high voltage, smaller rating of semiconductor devices and better feature of output voltage in term of less distortion, lower harmonics contents and lower switching losses. Furthermore, the complex phase shifting transformers that are needed in the multipulse inverters at higher level are not necessarily required, thus helps in reducing the cost, [12], [13].

The Space Vector Modulation (SVM) technique has gained wide acceptance for many AC drive applications, due to a higher DC bus voltage utilization (higher output voltage when compared with the SPWM), lower harmonic distortions and easy digital realization. In recent years, the SVM technique was extensively adopted in multilevel inverters since it offers greater numbers of

switching vectors for obtaining further improvements of AC drive performances. However, the use of multilevel inverters associated with SVM increases the complexity of control algorithm (or computational burden), in obtaining proper switching sequences and vectors, [14], [15], [16]. In this work, the input DC power supply of the multilevel inverter comes from a PWM rectifier with constant switching frequency.

In recent years, PWM rectifiers have been widely used in a variety of industrial applications due to their advanced qualities, such as absorption of sinusoidal current with low harmonic distortion and the possibility of operation with a power factor unity possibility of regeneration energy and DC-bus voltage control over a large range, [17], [18].

Many control strategies have been proposed for these PWM rectifiers. They can be classified into two categories [6-8], voltage oriented control (VOC) analogue to the vector control of electrical machines, and direct power control (DPC) analogue to the direct torque control of electrical machines. In this article we are interested in the application of Direct power control based on virtual flux with vector modulation (DPC-VF-SVM) , [19], [20]

In our case, in order to ensure better control of the voltages of the five-level inverter with NPC structure and obtain better performance, we propose a new type of frequency changer using a three-phase voltage rectifier with pulse width modulation .

Indeed, voltage rectifiers are taking an increasingly important place on the market today. They are mainly used as input stages for inverters in variable speed drives. The structure of the three-phase voltage rectifier with pulse width modulation makes it possible to obtain a minimum of harmonic distortions on the input current while ensuring an adjustable rectified voltage.

To this end, the expected objectives of this research work can be summarized in the following points:

1. Proposal for new frequency converters having the PWM three-phase voltage rectifier as an input stage of five-stage inverter with NPC structure and supplying a induction motor.

2. Development of control algorithms for the three-phase voltage rectifier PWM carried out by virtual flux-based direct control (DPC_VF) with vector modulation (SVM) allowing operation on a unit power factor on the network side and an adjustable output voltage in the two three-phase and two-phase markers.

3. Application of these algorithms for slaving the DC bus voltages of the frequency inverters offered.

Some other relevant studies can be found in [34], [35], [36], [37], [38].

2 Virtual flux based direct power control strategy

The increasing use of control systems based on industrial power electronics involves more and more disturbance problems at the level of the electrical power supply networks. Thus, a regular increase in current harmonic distortion and unbalance rates can be observed, as well as an important consumption of reactive power, [21]. Several solutions for reducing harmonic current in electrical power supply networks have been proposed. One of the interesting solutions is the use of a PWM rectifier, [22].

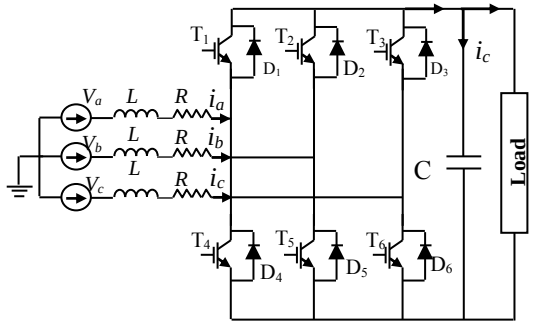

Figure 1: Three-phase PWM rectifier system

Many control strategies have been proposed for PWM rectifier, among them Direct Power Control (DPC), this command is developed by analogy with the direct torque control (DTC) of induction motors. It consists in controlling the instantaneous, active and reactive powers, instead of the torque and flux through two internal loops, [23], [24].

In this paper the virtual flux-based direct control (DPC_VF) with vector modulation (SVM) will be presented. This control strategy provides a high power factor and a quasi-sinusoidal waveform of the currents absorbed with a low THD while keeping the advantage of a control without line voltage sensor

The structure of the DPC_VF with vector modulation (SVM) is given by the following figure

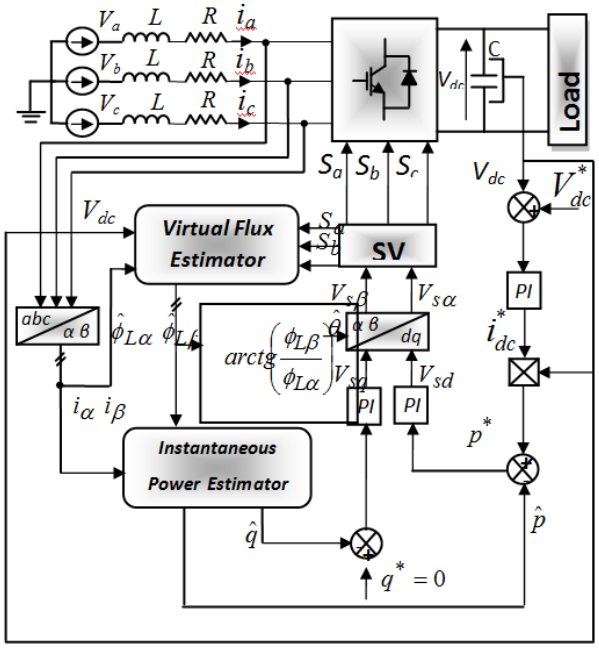

Figure 2: Basic diagram of DPC_VF with space vector modulation (SVM)

The virtual flux based approach has been proposed to improve the voltage-oriented control Here, it will be applied for instantaneous power estimation. The voltage imposed by the line power in combination with the ac-side inductors are assumed to be quantities related to a virtual ac motor as shown in Fig. 2. Thus, *R* and *L* represent the stator resistance and the stator leakage inductance of the virtual motor and phase-to-phase line voltages; *Vab* , *Vbc*, and *Vca* would be induced by a virtual air-gap flux

The components of the virtual flux are calculated from the following equations, [25]:

$$\hat{\phi}_{L\alpha} = \int (u_{s\alpha} + L\frac{di_\alpha}{dt})dt \tag{1}$$

$$\hat{\phi}_{L\beta} = \int (u_{s\beta} + L\frac{di_\beta}{dt})dt \tag{2}$$

We can write:

$$\hat{\phi}_{L\alpha} = L.i_\alpha + \int u_{s\alpha}dt \tag{3}$$

$$\hat{\phi}_{L\beta} = L.i_\beta + \int u_{s\beta}dt \tag{4}$$

Estimation of the instantaneous power based on the virtual flux, [22]:

$$\bar{\phi}_L = \begin{bmatrix} \phi_{L\alpha} \\ \phi_{L\beta} \end{bmatrix} = \begin{bmatrix} \int e_\alpha \\ \int e_\beta \end{bmatrix} \tag{5}$$

$$\bar{\phi}_c = \begin{bmatrix} \phi_{s\alpha} \\ \phi_{s\beta} \end{bmatrix} = \begin{bmatrix} \int u_{s\alpha} \\ \int u_{s\beta} \end{bmatrix} \tag{6}$$

The voltage equation is written in the following form, [26]:

$$\bar{e} = R\bar{i} + \frac{d}{dt}\left(L\bar{i} + \bar{\phi}_c\right) \tag{7}$$

In practice, the resistance ***R*** can be neglected, which gives

$$\bar{e} = \frac{d}{dt}\left(L\bar{i} + \bar{\phi}_c\right) \tag{8}$$

Using complex notation, instantaneous powers can be calculated as follows, [26]:

$$p = \mathrm{Re}\left(e.\bar{i}^*\right) \tag{9}$$

$$q = \mathrm{Im}\left(e.\bar{i}^*\right) \tag{10}$$

The line voltage can be expressed according to the virtual flux as follows, [26]:

$$\bar{e} = \frac{d}{dt}\bar{\phi}_L = \frac{d}{dt}\left(\phi_L e^{jwt}\right) = \frac{d\phi_L}{dt}e^{jwt} + jw\phi_L e^{jwt} = \frac{d\phi_L}{dt}e^{jwt} + jw\bar{\phi}_L \tag{11}$$

So the instantaneous active power is calculated by, [26]:

$$\hat{p} = \frac{d\phi_{Ld}}{dt}i_d + w\phi_{Ld}i_q \tag{12}$$

For a balanced three-phase sinusoidal voltage system, we have, [26]:

$$\frac{d\phi_{Ld}}{dt} = 0 \Rightarrow \hat{p} = w\phi_{Ld}i_q \tag{13}$$

Which means that only the component of the current orthogonal to the flux vector that produces the instantaneous active power

Similarly, the instantaneous reactive power can be calculated as follows, [26]:

$$\hat{q} = -\frac{d\phi_{Ld}}{dt} i_q + w\phi_{Ld} i_d \quad (14)$$

$$\frac{d\phi_{Ld}}{dt} = 0 \Rightarrow \hat{q} = w\phi_{Ld} i_d \quad (15)$$

The power estimator must use the quantities related to the stator α_β:

$$\bar{e} = \frac{d\phi_L}{dt}\bigg|_\alpha + j\frac{d\phi_L}{dt}\bigg|_\beta + jw\left(\phi_{L\alpha} + j\phi_{L\beta}\right) \quad (16)$$

$$\bar{e}.\bar{i}^* = \left\{\frac{d\phi_L}{dt}\bigg|_\alpha + j\frac{d\phi_L}{dt}\bigg|_\beta + jw\left(\phi_{L\alpha} + j\phi_{L\beta}\right)\right\}\left(i_\alpha - ji_\beta\right) \quad (17)$$

What allows to give, [26]:

$$\hat{p} = \frac{d\phi_L}{dt}\bigg|_\alpha .i_\alpha + \frac{d\phi_L}{dt}\bigg|_\beta .i_\beta + w\left(\phi_{L\alpha} i_\beta - \phi_{L\beta} i_\alpha\right) \quad (18)$$

$$\hat{q} = -\frac{d\phi_L}{dt}\bigg|_\alpha .i_\beta + \frac{d\phi_L}{dt}\bigg|_\beta .i_\alpha + w\left(\phi_{L\alpha} i_\alpha + \phi_{L\beta} i_\beta\right) \quad (19)$$

For sinusoidal and balanced line voltages, the derivatives of the flux are zero. Instantaneous active and reactive powers are calculated as follows, [26]:

$$\hat{p} = w\left(\phi_{L\alpha} i_\beta - \phi_{L\beta} i_\alpha\right) \quad (20)$$

$$\hat{q} = w\left(\phi_{L\alpha} i_\alpha + \phi_{L\beta} i_\beta\right) \quad (21)$$

3 Multilevel inverter

Multilevel inverters have been attracting attention in recent years due to high power quality, high voltage capability, low switching losses and low Electro Magnetic Interference (EMI) concerns; and have been proposed as the best choice in several medium and high voltage applications, [27], [28] , [29]. Among different topologies, the Neutral Point Clamped (NPC) inverter has received much attention, [30]. In this structure, diodes called floating diodes are associated with each phase, which serves to apply the different voltage levels of the DC source.

Moreover, abundant modulation techniques and control have been developed for multilevel inverter. Among them, space vector modulation is recognized as the most powerful and most used, [31].

3.1 Modeling of five-level inverter

Figure 3 shows the structure of the five-level inverter with NPC structure, each of the three arms of the inverter is composed of eight controlled switches, and six floating diodes. The controlled switches are unidirectional in voltage and bi-directional current, they are conventional associations of a transistor and an antiparallel diode.

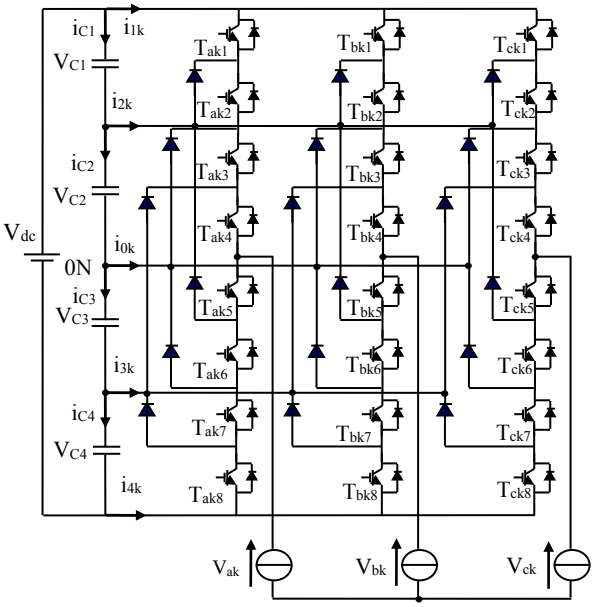

Figure 3: Structure of the five-level inverter with floating diodes

These switches must not be opened or closed simultaneously, in order to avoid a short circuit of the DC source of the input of the inverter, or the opening of the inductive circuit of its load.

The floating diodes (six per arm) ensure the application of the different voltage levels at the output of each arm. The continuous input bus is composed of four capacitors (C_1, C_2, C_3 and C_4), making it possible to create a set of three capacitive middle points. The total voltage of the DC bus is v_{dc}; under normal operating conditions, it is uniformly distributed over the four capacitors, which then have a voltage $v_{dc}/4$ at their terminals.

For each switch, T_{xki} (k=1, 2,3,4, i= 1… 8, x= *a, b* et *c*) a switching function is defined as follows:

$$F_{xki} = \begin{cases} 1 \; if \; T_{xki} \; is \; ON \\ 0 \; if \; T_{xki} \; is \; OFF \end{cases} \quad (22)$$

The switch commands of the lower half-arms are complementary to those of the upper half-arms:

$$F_{xki} = 1 - F_{xk(i-4)} \quad (23)$$

Table 1 summarizes the correspondence between the states of each arm, the states of its switches and its voltage output.

Switching State	State of the switches of an arm								Output voltage
	T_{xk1}	T_{xk2}	T_{xk3}	T_{xk4}	T_{xk5}	T_{xk6}	T_{xk7}	T_{xk8}	
4	1	1	1	1	0	0	0	0	$V_{c3}+V_{c4}$
3	0	1	1	1	1	0	0	0	V_{c3}
2	0	0	1	1	1	1	0	0	0
1	0	0	0	1	1	1	1	0	$-V_{c2}$
0	0	0	0	0	1	1	1	1	$-(V_{c1}+V_{c2})$

We define five connection functions, each associated with one of the five states of the arm:

$$\begin{cases} F_{c1xk} = F_{c1xk}F_{c2xk}F_{c3xk}F_{c4xk} \\ F_{c2xk} = F_{c2xk}F_{c3xk}F_{c4xk}F_{c5xk} \\ F_{c3xk} = F_{c3xk}F_{c4xk}F_{c5xk}F_{c6xk} \\ F_{c4xk} = F_{c4xk}F_{c5xk}F_{c6xk}F_{c7xk} \\ F_{c5xk} = F_{c5xk}F_{c6xk}F_{c7xk}F_{c8xk} \end{cases} \quad (24)$$

The potentials of the nodes a, b and c of the three-phase inverter at five levels with respect to the point "o" are given by the following system:

$$\begin{pmatrix} V_{aok} \\ V_{bok} \\ V_{cok} \end{pmatrix} = \begin{pmatrix} F_{c1ak} & F_{c2ak} & F_{c3ak} & F_{c4ak} & F_{c5ak} \\ F_{c1bk} & F_{c2bk} & F_{c3bk} & F_{c4bk} & F_{c5bk} \\ F_{c1ck} & F_{c2ck} & F_{c3ck} & F_{c4ck} & F_{c5ck} \end{pmatrix} \begin{pmatrix} V_{c3}+V_{c4} \\ V_{c3} \\ 0 \\ -V_{c2} \\ -(V_{c1}+V_{c2}) \end{pmatrix} \quad (25)$$

Thus, the input currents of the inverter are expressed as a function of the currents of the load i_{ak}, i_{bk} and i_{ck} by means of the connection functions of the half-arms by the following relations:

$$\begin{cases} i_{4k} = F_{ak4}i_{ak} + F_{bk4}i_{bk} + F_{ck4}i_{ck} \\ i_{3k} = F_{ak3}i_{ak} + F_{bk3}i_{bk} + F_{ck3}i_{ck} \\ i_{2k} = F_{ak2}i_{ak} + F_{bk2}i_{bk} + F_{ck2}i_{ck} \\ i_{1k} = F_{ak1}i_{ak} + F_{bk1}i_{bk} + F_{ck1}i_{ck} \\ i_{0k} = F_{ak0}i_{ak} + F_{bk0}i_{bk} + F_{ck0}i_{ck} \end{cases} \quad (26)$$

The five-level inverter has $5^3 = 125$ states, identified by the combination of states of the three arms. But in these 125 vectors there are redundant vectors, that is to say similar, among the 125 vectors we find 61 different vectors.

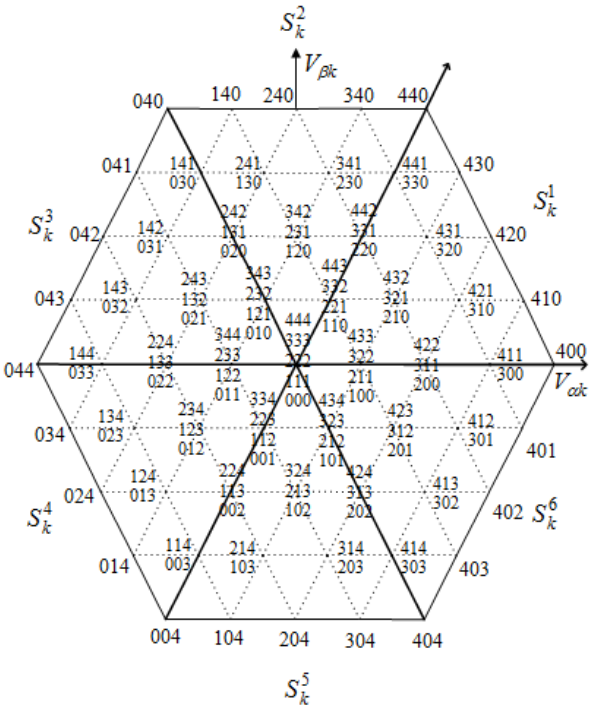

Figure 4: Vector diagram of the five level inverter.

There are 60 discrete positions, distributed over four hexagon, in addition to a position in the center of the hexagon. Some positions are created by several redundant states. From the outer hexagon to the inner hexagon, the positions of the voltage vector are created by one, two, three and four redundant states. The position of the center of the hexagon, which corresponds to a zero output voltage, is created by redundant states. We thus distinguish, [32]:

24 positions with one redundancy, 18 positions with two redundancies,12 positions with three redundancies and 6 positions with four redundancies.

The 61 positions of the output voltage vector divide the vector diagram into six triangular sectors. Each sector is composed of 16 triangular regions of Figure (4) so there are 96 triangular regions in the complete vector diagram.

3.2 SVM of the five-level inverter with floating diodes

Space vector modulation is a technique where the reference voltage is represented as a reference

vector to be generated by the inverter, [33] . SVM processes signals directly in the two-phase plane. It assumes that one works in the context of a numerical control and that a regulation algorithm has already determined the desired components $V_{ref\,\alpha k}$ and $V_{ref\,\beta k}$

The components projected on the two axes making 60°
between them are standardized by:

$$\begin{cases} V_{ref\,1k}^{S_k^1} = \dfrac{V_{refk}\cos(\varphi_k) - \dfrac{V_{refk}}{\sqrt{3}}\sin(\varphi_k)}{\sqrt{\dfrac{2}{3}}\dfrac{V_{dc}}{4}} \\ V_{ref\,2k}^{S_k^1} = \dfrac{\dfrac{2}{\sqrt{3}}V_{refk}\sin(\varphi_k)}{\sqrt{\dfrac{2}{3}}\dfrac{V_{dc}}{4}} \end{cases} \quad (27)$$

In each sector S_k^i, components $v_{ref\,1k}^{S_k^i}$ and $v_{ref\,2k}^{S_k^i}$ are given by:

$$\begin{cases} V_{ref\,1k}^{S_k^i} = 4M_k\left(\cos\left(\varphi_k - (S_k^i - 1)\dfrac{\pi}{3}\right) - \dfrac{1}{\sqrt{3}}\sin\left(\varphi_k - (S_k^i - 1)\dfrac{\pi}{3}\right)\right) \\ V_{ref\,2k}^{S_k^i} = 4M_k\left(\dfrac{2}{\sqrt{3}}\sin\left(\varphi_k - (S_k^i - 1)\dfrac{\pi}{3}\right)\right) \end{cases} \quad (28)$$

To determine the number of the triangle in a sector S_k^i, the following two integers are to be defined:

$$\begin{cases} l_{1k}^{S_k^i} = \text{int}\left(V_{ref\,1k}^{S_k^i}\right) \\ l_{2k}^{S_k^i} = \text{int}\left(V_{ref\,2k}^{S_k^i}\right) \end{cases} \quad (29)$$

Where, 'int' is a function that gives the integer part of a given real number.
The triangular regions of the five-level inverter.

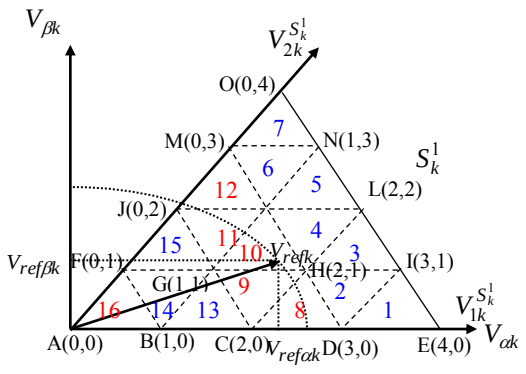

Figure 5: Coordinates of the different vertices of the triangles in a sector S_k^i

if the reference vector is in the parallelogram formed by the vertices G, H, K and L, as shown in Figure (5), the following two conditions must be verified:

V_{refk} is in the triangle (GHK) if:

$$V_{ref\,1k}^{S_k^i} + V_{ref\,2k}^{S_k^i} < l_{1k}^{S_k^i} + l_{2k}^{S_k^i} + 1 \quad (30)$$

V_{refk} is in the triangle (KHL) if:

$$V_{ref\,1k}^{S_k^i} + V_{ref\,2k}^{S_k^i} \geq l_{1k}^{S_k^i} + l_{2k}^{S_k^i} + 1 \quad (31)$$

To calculate the application times and as an example, if the reference vector is in the triangle 10 $\Delta_{10}^{S_k^1}$ it can then be reconstituted from the three adjacent vectors $V_x^{\Delta_{10}^{S_k^1}}$, $V_y^{\Delta_{10}^{S_k^1}}$ and $V_z^{\Delta_{10}^{S_k^1}}$ using the following relation:

$$\begin{cases} V_x^{\Delta_{10}^{S_k^1}} t_x^{\Delta_{10}^{S_k^1}} + V_y^{\Delta_{10}^{S_k^1}} t_y^{\Delta_{10}^{S_k^1}} + V_z^{\Delta_{10}^{S_k^1}} t_z^{\Delta_{10}^{S_k^1}} = V_{ref} T_s \\ t_x^{\Delta_{10}^{S_k^1}} + t_y^{\Delta_{10}^{S_k^1}} + t_z^{\Delta_{10}^{S_k^1}} = T_s \end{cases} \quad (32)$$

Where $t_x^{\Delta_{10}^{S_k^1}}$, $t_y^{\Delta_{10}^{S_k^1}}$ and $t_z^{\Delta_{10}^{S_k^1}}$ are the application times of the vectors $V_x^{\Delta_{10}^{S_k^1}}$, $V_y^{\Delta_{10}^{S_k^1}}$ and $V_z^{\Delta_{10}^{S_k^1}}$ respectively, and x, y and z are the vertices of G, H and K respectively.

$\Delta_{10}^{S_k^i}$ is number of the triangle 'i' located in a sector S_k^i

To calculate the application times, equation (32) is decomposed according to the two axes $V_{1k}^{S_k^i}$ and $V_{2k}^{S_k^i}$ as follows:

$$\begin{cases} V_{x1}^{\Delta_{10}^{S_k^1}} t_x^{\Delta_{10}^{S_k^1}} + V_{y1}^{\Delta_{10}^{S_k^1}} t_y^{\Delta_{10}^{S_k^1}} + V_{z1}^{\Delta_{10}^{S_k^1}} t_z^{\Delta_{10}^{S_k^1}} = V_{ref\,1} T_s \\ V_{x2}^{\Delta_{10}^{S_k^1}} t_x^{\Delta_{10}^{S_k^1}} + V_{y2}^{\Delta_{10}^{S_k^1}} t_y^{\Delta_{10}^{S_k^1}} + V_{z2}^{\Delta_{10}^{S_k^1}} t_z^{\Delta_{10}^{S_k^1}} = V_{ref\,2} T_s \\ t_x^{\Delta_{10}^{S_k^1}} + t_y^{\Delta_{10}^{S_k^1}} + t_z^{\Delta_{10}^{S_k^1}} = T_s \end{cases} \quad (33)$$

The substitution of vector coordinates $V_x^{\Delta_{10}^{S_k^1}} = V_G^{\Delta_{10}^{S_k^1}}$, $V_y^{\Delta_{10}^{S_k^1}} = V_H^{\Delta_{10}^{S_k^1}}$ and $V_z^{\Delta_{10}^{S_k^1}} = V_K^{\Delta_{10}^{S_k^1}}$ in equation (33) makes it possible to calculate the application times of these vectors as follows:

$$\begin{cases} t_y^{\Delta_{10}^{S_k^1}} = \left(V_{ref1k}^{S_k^1} - l_{1k}^{S_k^1}\right)T_s \\ t_z^{\Delta_{10}^{S_k^1}} = \left(V_{ref2k}^{S_k^1} - l_{2k}^{S_k^1}\right)T_s \\ t_x^{\Delta_{10}^{S_k^1}} = T_s - \left(t_y^{\Delta_{10}^{S_k^1}} - t_z^{\Delta_{10}^{S_k^1}}\right) \end{cases} \quad (34)$$

4 Results and analysis

In this paper, instead of using a classic rectifier to feed the five-level inverter , we use a PWM rectifier. The latter improves the quality of the output DC voltage of the rectifier with a reduced switching frequency. Additionally, its input AC voltage and current are very less polluted than those of classic rectifier.

The first part of the simulation was dedicated to investigating the performance of the PWM rectifier based virtual flux estimator with vector modulation (SVM). The second part of the simulation was devoted to testing the performance of a 5-level Neutral point clamped inverter with DPC-VF-SVM Rectifier as power source.

For the validation of the proposed DPC strategy PWM rectifier, the system has been modelled and built in MATLAB/SIMULINK software environment and tested under various conditions.

The main electrical parameters of the system are given in table1.

Table 1. Parameters of the power circuit

Line resistance	*R=0.25 Ω*
Line inductance	*L=10 mH*
The capacitor	*C=5 mF*
Load resistance	R_{ch}*=100 Ω.*
Source voltage frequency	*50 Hz*
Peak amplitude of line voltage	$\sqrt{2}$ *220 V.*
DC-Voltage Reference	V_{dc}*= 600 V*

The simulation results obtained are illustrated in the figures below:

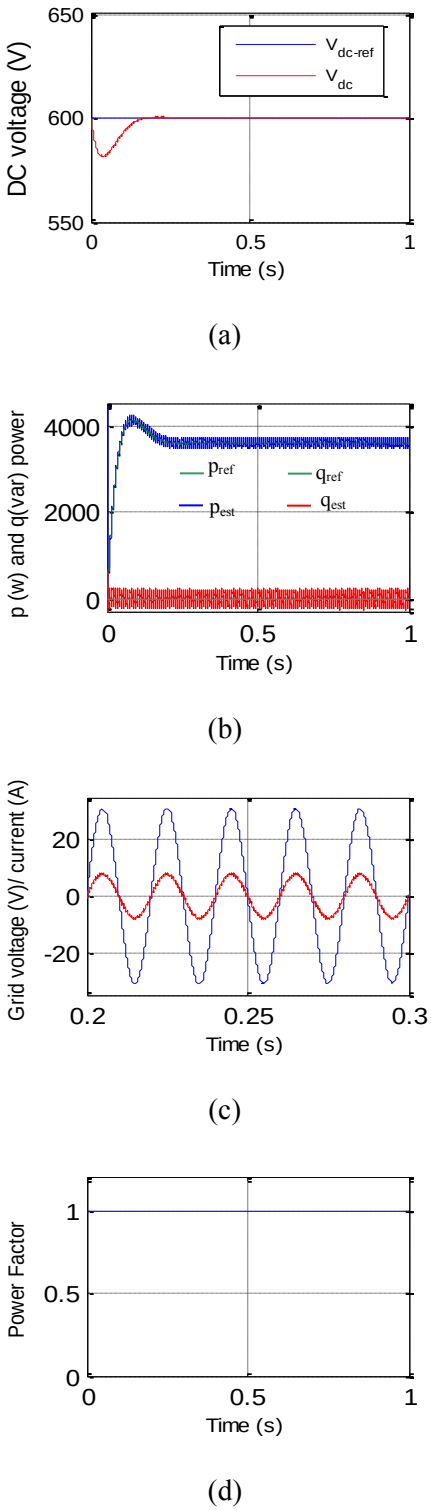

Figure 6: Performance of the DPC_VF_SVM of a PWM rectifier: DC output voltage (a); Active and reactive power (b); Voltage and current waveforms of phase 'a' (c); Power Factor (d)

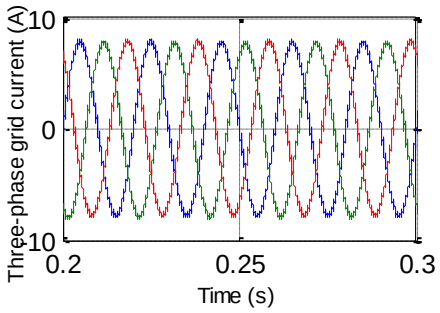

Figure 7: Zoom of line current

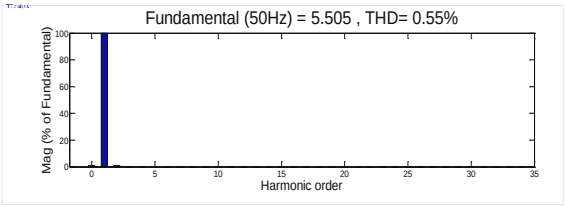

Figure 8: Line current harmonics spectrum

The DC voltage follows its reference well with a certain transient overrange (Figure 6.a), The active and reactive powers estimated follow perfectly their references (Figure 6.b). The absorbed currents are in phase with the grid line voltages that provide a unity power factor (Figures 6.c and d).The line current is substantially sinusoidal with a low harmonic distortion ratio THD equal to: 0.55% (Figures 7 and 8).

To test the robustness of the proposed technique (DPC_VF_SVM) and in order to show these dynamic performances, we have varied the reference DC voltage from 600 V to 700 V at t=0.5s, we notice that the active power and the line current increase when the voltage continues reached its new reference, while the reactive power and the DC voltage remain locked to their references (Figures 9). This is due to the good regulation of the DC voltage. The results show that the proposed solution allows the use of this topology to compensate for the harmonic current and the reactive power in high-power utilities.

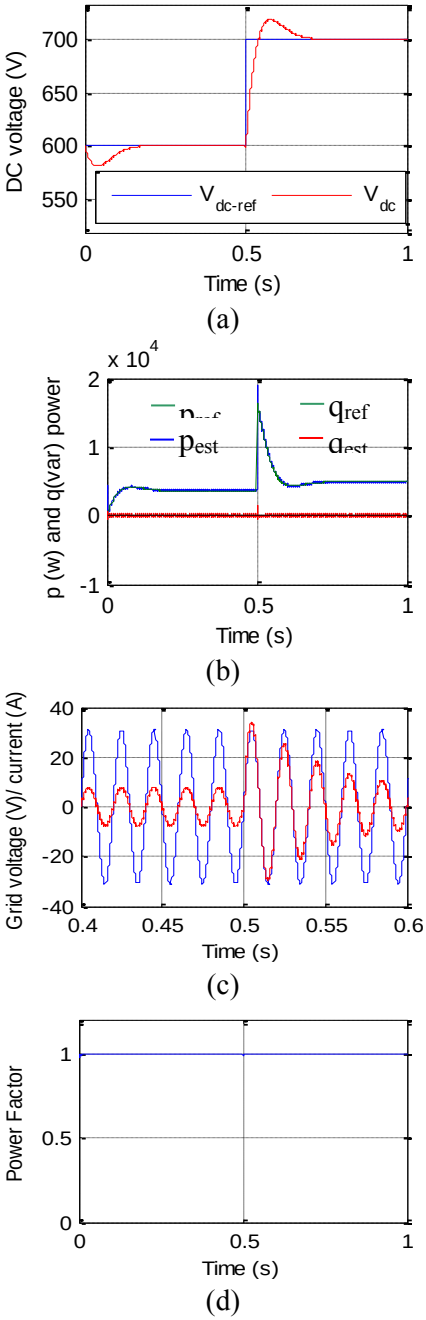

Figure 9: Performance of the DPC_VF_SVM of a PWM rectifier during a variation of the reference voltage from 600V to 700V at t = 0.5s: DC output voltage (a); Active and reactive power (b); Voltage and current waveforms of phase 'a' (c); Power Factor (d)

Fig. 10 shows the cascade control scheme for a three-phase electrical network, a two-level rectifier, a five-level inverter and an induction motor. The rectifier and the inverter are controlled in vector modulation.

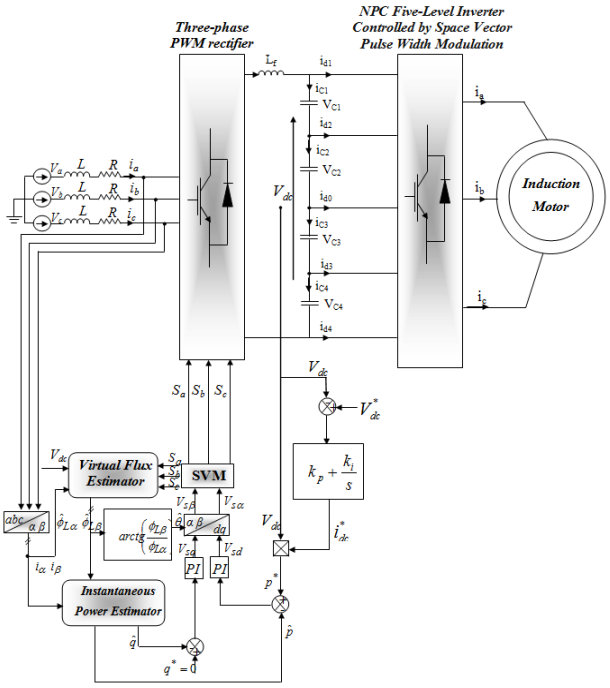

Figure 10: Cascade control diagram three-phase network - 2-level rectifier - 5-level inverter - Induction Motor

The proposed cascade control model is implemented in MATLAB/SIMULINK software.

Figure 11 show switching pulse generation using SVM control. This simulation results show that the proposed SVM technique significantly out-performs the traditional PWM in terms of decreasing the number of commutations of switches.

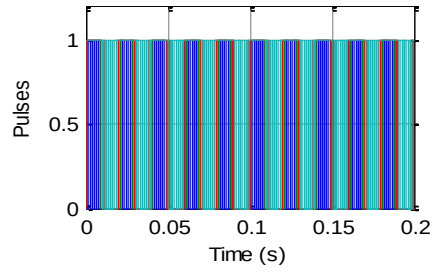

(a)

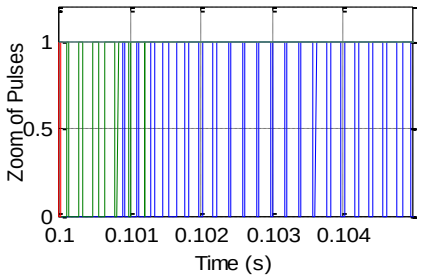

(b)

Figure 11: Switching pulse generation using SVM control

The charging currents for five level inverter using SVM by DPC-VF-SVM Rectifier as DC source is shown in figure12, three phase current is obtained and each is having a phase delay of 120°. We notice that these currents are sinusoidal which gives a low rate of harmonic distortion.

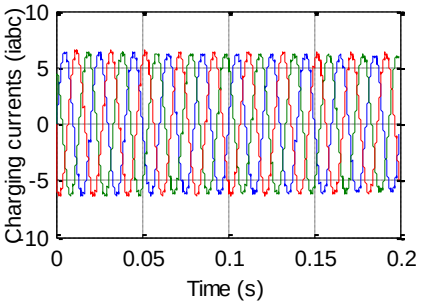

(a)

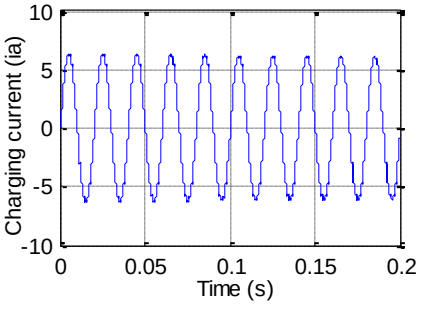

(b)

Figure 12: Charging currents for the five-level inverter

Figures (13) and (14) show the output voltages of the first phase and the FFT plot for out-put voltage of five level NPC inverter fed by DPC-VF-SVM rectifier. From the figure it is clear that output THD obtained from the SVM technique result in less distortion.

The simulation results confirm that the use of five level NPC inverter using SVM control fed by DPC-VF-SVM rectifier gives enhanced fundamental output with better quality i.e. lesser THD.

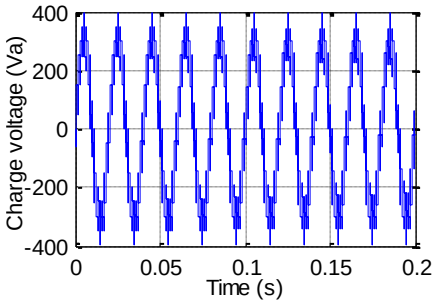

(a)

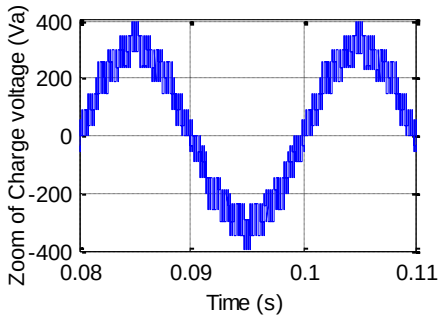

(b)

Figure 13: Output voltages for the five-level inverter

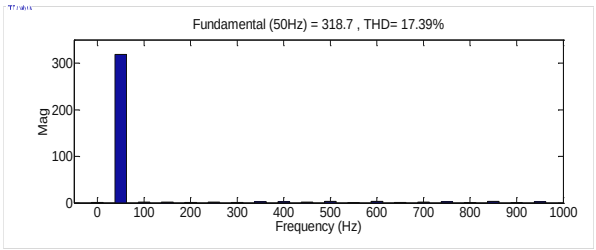

Figure 14: Harmonic spectrum of the output voltage

The induction motor (IM) is supplied by a five-level floating diode inverter, which is supplied by a three-phase PWM voltage rectifier as an input stage in order to improve the spectrum of output voltages.

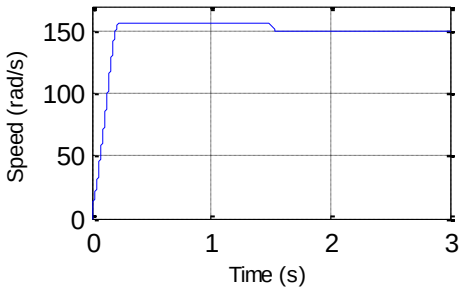

(a) The motor speed

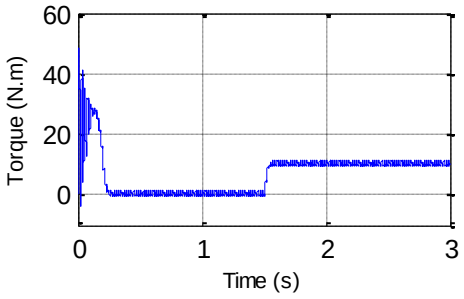

(b) The motor torque

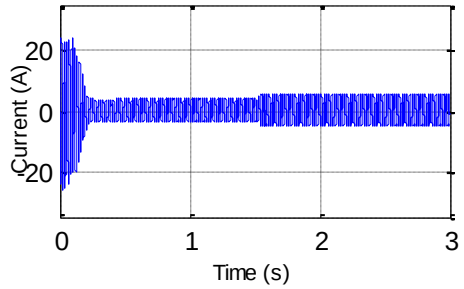

(c) The output current

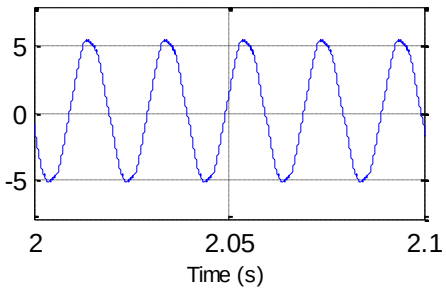

(d) The zoom of output current

Fig. 15. Results of Five-Level inverter fed induction motor

The speed curve shown in Figure 15(a) has three sections; transient state section from 0 to 0.24 s, no load operation section from 0.24-1.5 s and a section for load (10 N.m) operation applied at 1.5 s. The torque curve presented in Figure 15(b) has three sections; transient state section from 0 to 0.25 s, no load (0.00 N.m) operation section from 0.25-1.5 s and a section for load (10 N.m) operation applied at 1.5s. It can be observed that speed and torque time responses are better when the motor is fed by five-level inverter. The inverter output current waveform of five-level inverter is almost sinusoidal contains less harmonics and less torque fluctuations thus, a better motor dynamic response is obtained. The results have showed that when five level inverter supplied by a three-phase PWM voltage rectifier as an input stage is used the harmonic currents and voltage distortions are reduced and torque fluctuations are less.

5 Conclusion

In this paper, in the first part a robust DPC control was presented, based on virtual flux estimator for a better control of the PWM rectifier. The effectiveness of this control was obtained by correcting the active and reactive power at the same time and it can be found that its are independent of each other. Moreover, the result shows that the THD of the source current is 0.55% and this control ensures a power factor equal to unity. The second part has presented a study of five level inverter topologie controlled by space vector PWM, which is supplied by a three-phase PWM voltage rectifier as an input stage, feeding an induction motor. The results have showed that five level inverter gives reduced harmonics current and voltage distortion and less torque fluctuations.

References:

[1] A. H.Wahidah, S. Ganeson, M.Azri, T.N.A.Tengku Azam, "Review of Multilevel Inverter Topologies and Its Applications", Journal of Telecommunication, Electronic and Computer Engineering, 8(7), pp. 51-56, 2016

[2] S.Tahir, J. Wang, B. M. Hussain, K. G. Sarwar, "Digital control techniques based on voltage source inverters in renewable energy applications: A Review", Electronics, 7(18), pp. 1-37, 2018.

[3] S. Kouro, M. Malinowski, K. Gopakumar, J. Pou, G. Franquelo, B. Wu, J. Rodriguez, M. A. Pérez, J. I. Leon, "Recent advances and industrial applications of multilevel converters", IEEE Transactions on Industrial Electronics, 57(8), pp. 2553-2580, 2010.

[4] S. Busquets-Monge, J. Rocabert, P. Rodríguez, S. Alepuz, J. Bordonau, "Multilevel diode-clamped converter for photovoltaic generators with independent voltage control of each solar array", IEEE Transactions on Industrial Electronics, 55(7), pp. 2713-2723, 2008.

[5] A. R. Ronak, A. Sujal, M. Anand, w.L. Chee, K. Hee-Je, "Review of Multilevel Voltage Source Inverter Topologies and Analysis of Harmonics Distortions in FC-MLI", electronics, 8, 1329,pp: 1-37, 2019

[6] B. Li, S. Zhou, D. Xu, R. Yang, D. Xu, C. Buccella, C. Cecati, "An improved circulating current injection method for modular multilevel converters in variable-speed drives", IEEE Transactions on Industrial Electronics, pp. 1-10, (2016).

[7] S. G. Shehu, A. B. Kunya, I. H. Shanono, T. Yalcinoz, "A review of multilevel inverter topology and control techniques", Journal of Automation and Control Engineering, 4(3), pp. 233- 241, 2016.

[8] H. Kazunori, A. Hirofumi, "A new DC-voltage-balancing circuit including a single coupled inductor for a five-level diode-clamped PWM inverter", IEEE Transactions on Industry Applications, 47(2), pp. 841-852, 2011.

[9] J. Ebrahimi, E. Babaei, G. B. Gharehpetian " A new multilevel converter topology with reduced number of power electronic components, " IEEE Trans. Ind. Electronics., vol. 59, NO.2 pp. 655-667,Feb 2012.

[10] B. S. Muhammad, H. Ammar, I. A. Mian, "A New Multilevel Inverter Topology for Grid-Connected Photovoltaic Systems", Hindawi, International Journal of Photoenergy, pp: 1-9, 2018

[11] R. P. Sridhar, K. Georgios, G. A. Vassilios, "Hybrid seven-level cascaded active neutral-point-clamped-based multilevel converter under SHE-PWM", IEEE Transactions on Industrial Electronics, 60(11), pp. 4794-4804, 2013.

[12] N. Ehsan, M. Y. Abdul Halim, "Design and implementation of a new

multilevel inverter topology", IEEE Transactions on Industrial Electronics, 59(11), pp. 4148-4154, 2012.

[13] K. S. Arash, D. Vahid, A. Mostafa, D. Saeedeh, "Reduced DC voltage source flying capacitor multicell multilevel inverter: analysis and implementation", IET Power Electronics, Vol. 7, Iss. 2, pp. 439-450, 2014.

[14] J. Biji, M. R. Baiju, "A New Space Vector Modulation Scheme for Multilevel Inverters which Directly Vector Quantize the Reference Space Vector ", IEEE TRANSACTIONS ON INDUSTRIAL ELECTRONICS, pp: 1-8, 2013

[15] T. Xiongmin, Z. Junhui, L. Zheng, Z. Miao, "A switching frequency optimized space vector pulse width modulation (SVPWM) scheme for cascaded multilevel inverters", Energies, 10, pp. 1-18, 2017.

[16] B. M. Zouhaira, H. Mahmoud, M. Hamdi, "Space vector modulation of multilevel inverters: a simple and fast method of two-level hexagon's selection", International Journal Power Electronics, 8(2), pp. 107-123, 2017.

[17] A. Draou, "A space vector modulation based three-level PWM rectifier under simple sliding mode control strategy", Energy and Power Engineering, 5, pp. 28-35, 2013.

[18] A. K. Davood, N. Amir, "Design and simulation of a PWM rectifier connected to a PM generator of micro turbine unit", Scientia Iranica, Transactions D: Computer Science & Engineering and Electrical Engineering, 19 (3), pp: 820-828, 2012

[19] Z. E. LAGGOUN, H. BENALLA, K. NEBTI," Dual virtual flux-based direct power control for rectifier under harmonically distorted voltage condition", ARCHIVES OF ELECTRICAL ENGINEERING, VOL. 69(4), pp. 951–966, 2020

[20] B. Wenshao, X. Leilei, "Direct power control strategy of PWM rectifier based on improved virtual flux-linkage observer", Hindawi Journal of Control Science and Engineering, pp.1-9, 2017.

[21] A. Bechouche, H. Seddiki, D.O. Abdeslam, A. Rahoui, Y. Triki, P. Wira, "Predictive direct power control with virtual-flux estimation of three-phase PWM rectifiers under nonideal grid voltages", in 2018 IEEE International Conference on Industrial Technology (ICIT), France, Lyon, pp. 806–811, 2018

[22] M. Malinowski, M. Jasinski, M. P. Kazmierkowski, "Simple direct power control of three-phase PWM rectifier using space-vector modulation (DPC-SVM) ", IEEE Transactions on Industrial Electronics, 51(2), 2004.

[23] M. A. Razali, M. A. Rahman, "Performance analysis of three-phase PWM rectifier using direct power control", IEEE International Electric Machines & Drives Conference (IEMDC), pp. 16033-1605, 2011.

[24] Y. Zhang, Z. Li, Y. Zhang, W. Xie, Z. Piao, C. Hu, "Performance improvement of direct power control of PWM rectifier with simple calculation", IEEE Transactions on Power Electronics, 28(7), pp. 3428-3437, 2013.

[25] A. Rahab, F. Senani, H. Benalla, "Direct power control of three phase PWM rectifier based DSOGI-VF estimator for no-Ideal line voltages conditions", International Journal of Engineering Research and Application, 8(1), (Part -1), pp.10-18, 2018.

[26] M. Malinowski, M. P. Kazmierkowski, S. Hansen, F. Blaabjerg, G. D. Marques, "Virtual-flux-based direct power control of three-phase PWM rectifiers", IEEE Transactions on Industry Applications, 37(4), 2001.

[27] Z. Jianzhong, X. Shuai, D. Zakuid, H. Xing, "Hybrid Multilevel Converters: Topologies, Evolutions and Verifications", energies, 12(615), pp: 1-29, 2019.

[28] A. Bughneda, M. Salem, A. Richelli, I. Dahaman, S. Alatai, "Review of Multilevel Inverters for PV Energy System Applications", energies, 14(1585), pp: 1-23, 2021.

[29] M. Malinowski, K. Gopakumar, J. Rodriguez, M. A. Pérez, "A survey on cascaded multilevel inverters", IEEE Transactions on Industrial Electronics, 57(7), pp. 2197-2206, 2010.

[30] S. D. D. Banerjee, K. Siva kumar, K. Gopakumar, R. Ramchand, C. Patel, "Multilevel inverters for low-power application", IET Power Electron., 4(4), pp. 384–392, 2011.

[31] M. M. Hasan, S. Mekhilef, T. Messikh, M. Ahmed, "Three-phase

multilevel inverter with high value of resolution per switch employing a space vector modulation control scheme", Turkish Journal of Electrical Engineering & Computer Sciences; (34), pp. 1993-2009, 2016.

[32] K. Satyanarayana, B. Anjaneyulu, K. S. Prasad, "Performance improvement of multi level inverter fed vector controlled induction motor drive for low speed operations", International Journal of Power Electronics and Drive System (IJPEDS); 4(1), pp. 51-60, 2014.

[33] S. Syamim, J. Auzani, S. Tole, A. K. Kasrul, M. J. Mohd Luqman, A. T. Siti Azura "Implementation of Space Vector Modulator for Cascaded H-Bridge Multilevel Inverters", International Journal of Power Electronics and Drive System (IJPEDS), 6(4), pp. 906-918, 2015.

[34] H. Denoun, N. Benamrouche, S. Haddad, S. Meziani and S. Ait mamar, "A D.S.P (TMS320lf2407) based implementation of P.W.M for single-phase ACDC bipolar converter with a unity power factor", International Journal on Circuits, Systems and Signal Processing, pp.354-361, Issue 4, Volume 5, 2011

[35] Wei Huang, Power System Frequency Prediction after Disturbance based on Deep Learning, International Journal on Circuits, Systems and Signal Processing, pp. 716-725, Volume 14, 2020

[36] Qiaoli He, "Harmonics of Double-fed Wind Power System with Grid-Tied Dual-PWM Converter", International Journal on Circuits, Systems and Signal Processing, pp. 743-750, Volume 14, 2020

[37] Sufen Li, "Short-Term Load Forecasting of Power System Based on Improved BP Neural Network", International Journal on Circuits, Systems and Signal Processing, pp. 840-846, Volume 14, 2020

[38] Candidus U. Eya, Ayodeji Olalekan Salau, Stephen Ejiofor Oti, "High Performance DC-to-AC Converter using Snubberless H-Bridge Power Switches and an Improved DC-to-DC Converter", International Journal on Circuits, Systems and Signal Processing, pp. 315-333 , Volume 15, 2021